ELSEVIER

Journal of Photochemistry and Photobiology A: Chemistry 131 (2000) 17–21

Journal of Photochemistry and Photobiology A:Chemistry

www.elsevier.nl/locate/jphotochem

Photophysics of a phenyl-pyridinium cation with hindered rotation

V.A. Kharlanov[a,*,1], M.I. Knyazhansky [a], A.V. Bicherov [a], W. Rettig [b]

[a] *Institute of Physical and Organic Chemistry, Rostov State University, Stachka str. 194/2, Rostov on Don, 344090, Russia*

[b] *Institute of Physical and Theoretical Chemistry, Humboldt University of Berlin, Bunsenstr. 1, 10117 Berlin, Germany*

Received 14 October 1999; accepted 20 October 1999

Abstract

The influence of the internal rotation on the photophysical parameters of the pyridinium cation *N*-methyl-9-phenyl-1,2,3,4,5,6,7,8-octahydroacridinium **9PA** was studied by absorption and fluorescence spectroscopy as well as by semiempirical calculations. A weak long wavelength absorption shoulder at 340 nm appears in the red edge of longest wavelength absorption band and is caused by a forbidden transition of charge transfer nature involving the phenyl group as the electron donor. The excitation of **9PA** at any point of the absorption spectrum leads to a weak ($\Phi_f = 0.03$) fluorescence at 420 nm possessing a relatively large Stokes shift with respect to the weak long wavelength absorption shoulder ($\Delta\nu_{a\text{-}f} = 5600\,cm^{-1}$) and a long fluorescence lifetime (average decay time 5.4 ns). The fluorescence corresponds to a forbidden transition from the twisted S_1 state equilibrium geometry generated from the more twisted S_1-Frank-Codon geometry. ©2000 Published by Elsevier Science S.A. All rights reserved.

Keywords: Internal hindered rotation; Phenyl pyridinium cations; Semiempirical calculation; Absorption; Fluorescence spectroscopies

1. Introduction

It was shown by us earlier and in recent work [1–3] that in the 2,4,6-triphenylpyridinium cation **TPP**, the longest wavelength transition in absorption ($\lambda_a \approx 330$ nm) corresponding to the intramolecular charge transfer (CT) from the non-planar 2,6-aryl rings (the torsional angles are 50–60°) into pyridinum moiety promotes the adiabatic structural relaxation connected with the rotation of the 2,6-aryl rings resulting in the formation of a flattened structure responsible for the fluorescence with anomalously large Stokes shift ($\Delta\nu_{a\text{-}f} \approx 10\,000\,cm^{-1}$).

At the same time, the shorter wavelength transition ($\lambda_a \approx 290$ nm) is connected with CT from the considerably flattened (the torsional angle is 10–20°) 4-phenyl into the pyridinium ring, and it is not directly responsible for the adiabatic relaxation and Stokes shift. However, this transition plays an appreciable role in the fluorescent properties of these cations. Nevertheless, the mechanism of this influence is almost unexplored. One can expect that the properties of this electronic transition in absorption and emission should depend on the non-coplanarity of the 4-phenyl group. This expectation is supported by the fact that the 1-methyl-4-phenylpyridinium cation **1M4PPY**, where free rotation is possible, possesses a smaller Stokes shift ($3480\,cm^{-1}$) than **TPP** [4].

To take more clear view of the 4-phenyl ring twist angle effect, detailed studies of the photophysical parameters for the model pyridinium cation *N*-Methyl-9-phenyl-1,2,3,4,5,6,7,8-octahydroacridinium **9PA** containing the single nearly perpendicular phenyl fragment with hindered rotation have been carried out by the experimental and quantum chemical methods.

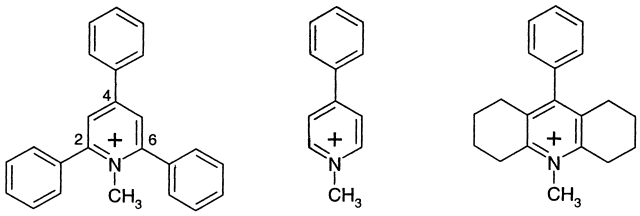

TPP **1M4PPY** **9PA**

2. Experimentals details

2.1. Materials

9PA was prepared in the form of the borftoride salt (anion BF_4^-) by known methods [5] and purified by recrystalliza-

* Corresponding author. Fax: +7-8632-285667.

E-mail addresses: vlad@ipoc.rnd.runnet.ru (V.A. Kharlanov), vlad@asterix.chemie.hu-berlin.de (V.A. Kharlanov).

[1] Fax: +4930-2093-5574.

1010-6030/00/$ – see front matter
PII: S1010-6030(99)00218-X

tion. The product was checked for purity by fluorescence after each recryrstallization step as in a previous paper [6]. The solvent (ethanol) used was of spectroscopic grade quality (MERCK UVASOL).

2.2. Apparatus and methods

Absorption spectra were recorded with a ATI Unicam UV2 spectrophotometer (UK). Corrected fluorescence emission and fluorescence excitation spectra of solutions with an absorbance $A = 0.02$–0.06 were measured with a SLM AMINCO AB2 spectrofluorimeter.

Fluorescence quantum yields (±10%) were determined using naphthalene in cyclohexane as standard ($\Phi_f = 0.23 \pm 0.02$ [7]). The refractive index corrections were made [8] (Table 3.1) to adjust for the different solvents used. The quantum yield changes with temperature variation were corrected both with respect to the refractive index [9] and density [10] changes of the solvent.

The fluorescence lifetime measurements were performed with a single photon counting equipment using synchroton radiation in the single bunch mode from the Berlin storage ring BESSY is the excitation source, as described elsewhere [11]. The excitation wavelength ($\Delta\lambda = 20$ nm) was chosen at 284 nm (S_2-state, $A = 0.02$–0.06). The decay times were fitted using the iterative reconvolution technique which allowed a time resolution down to 0.1 ns and a precision of better than 0.1 ns. Satisfactory fits ($\chi^2 < 1.2$) were obtained in all cases with 1 or 2 exponential terms.

2.3. Methods of calculations

The ground and excited state calculations were carried out with full geometry optimization using the AM1 [12] implementation in AMPAC 5.0 [13]. The optimization was performed using the Newton algorithm with vibrational analysis of the optimized structure for a determination of stable and transition geometries. The calculation of the potential energy surface of internal rotation were carried out by fixing the angle between the fragments and optimizing all other geometrical parameters.

The calculation of transition energies and oscillator strengths were carried out using the CNDO/S-CI method with interaction of 50 singly excited configurations and the parameter sets described in [14–21] for the fully optimized AM1 ground state structures.

3. Results and discussion

3.1. Absorption spectra

The absorption spectrum of **9PA** (Fig. 1 and Table 1) is represented by two bands, the positions and intensities of which are similar to those of the alkyl substituted pyridinium

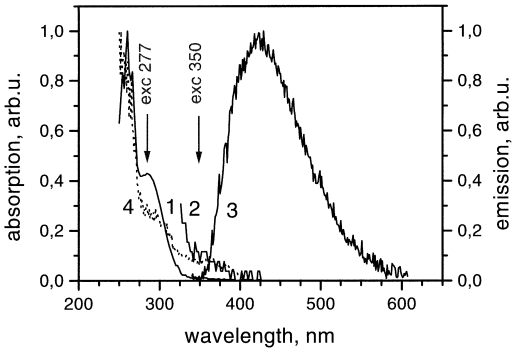

Fig. 1. The absorption spectrum (1) with the edge of the long wavelength absorption band (× 100), (2), the corrected fluorescence spectrum (identical for excitation at 277 and 350 nm) (3) and the fluorescence excitation spectrum (observation at 420 nm) (4) of **9PA** (ethanol, 296 K).

cations [22–24]. The small influence of the phenyl group in the 9-position of the heteroaromatic ring on the absorption spectrum shows that both fragments are orthogonal to each other because of the steric interaction of the phenyl ring with the methylene chains. In the red edge of the long wavelength absorption band, a weak absorption is displayed as a shoulder (Fig. 1, Table 1), the investigation of which is difficult due to the very small solubility of the salt studied. It may be assumed that the weak absorption is of charge transfer (CT) nature with electron transfer from the phenyl group to the heteroring. To elucidate the structure of the cation and the nature of the electronic transitions in the absorption spectra, quantum chemical calculations by the semiempirical methods AM1 and CNDO/S have been carried out.

3.2. Quantum chemical calculations

According to the semiempirical calculations by the AM1 method, the cation **9PA** is of near orthogonal geometry (the torsional angle in 82.9°) in the S_0 state. This orthogonal arrangement (Fig. 2, Table 2) is consistent with the behavior of another pyridinium system with strong sterical hindrance as evidenced by the experimental [25,26] and calculational results [27].

The study of the nature of the electronic transitions by CNDO/S for the calculated equilibrium geometry of **9PA** supports the view that the electronic transitions are separated into transitions localized on the different fragments (the locally excited transition LE) and transitions with CT nature (Table 3). The corresponds to a principle formulated previously for other systems with nearly orthogonal fragments

Table 1
Absorption bands[a] of **9PA** (ethanol, 298 K)

ΔE (eV)	3.64[b]	4.36	4.77
λ_a (nm)	340	284	260

[a] The molar extinction coefficient could not be determined because of the *v*.

[b] The orientation of the axes is shown in Fig. 2.

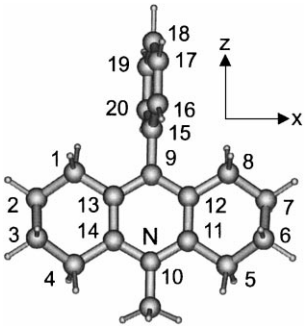

Fig. 2. Structure, axes and the atom numbers of **9PA** (equilibrium geometry of the S_0 state by AM1).

Table 2
Some bond lengths and dihedral angles for the S_0 equilibrium geometry (AM1) or **9PXANT** (The number of the atoms are given in Fig. 2)

Bond length (Å)	Dihedral angle (°)
10–11	1.3805
11–12	1.4113
9–12	1.4084
9–15	1.4677
15–16	1.4015
16–17	1.3934
17–18	1.3953
12–9–15–16	82.9

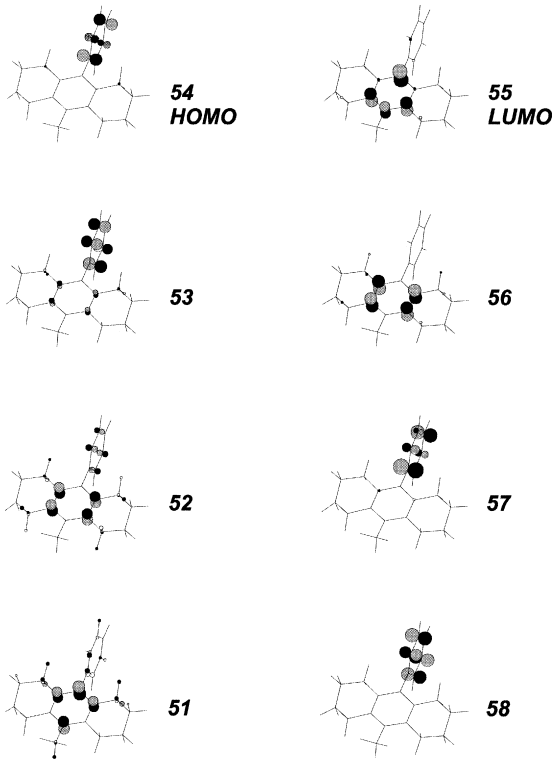

Fig. 3. The occupied (left) and unoccupied (right) molecular orbitals (CNDO/S) involved in the lowest singlet and triplet excited states of **9PA** (for the S_0 equilibrium geometry).

[27]. The weak interaction between the fragments results in the localization of the molecular orbitals on the different fragments (Fig. 3) and the transitions among the orbitals allow a clear distinction of these two types of states.

The results of the calculation (Table 3 and Fig. 3) show that the weak long wavelength absorption band corresponds to a forbidden transition $S_0 \rightarrow S_1$ ($f = 0.0198$) connected with the transfer of an electron from the phenyl group to the acridinium ring. Basically, this transition is formed by an interaction of the molecular orbitals 54 (HOMO) and 55 (LOMO) localized on the different fragments (Fig. 3).

Further analysis of the results (Table 3 and Fig. 3) shows that the absorption bands with $\lambda_a = 284$ and 240 nm are caused by the LE transitions $S_0 \rightarrow S_2$ and $S_0 \rightarrow S_8$, respectively. Both transitions are localized on the acridinium fragment and possess a different orientation of the transition dipole moment (axes *x* and *z*, respectively, Fig. 2). The other transitions from $S_0 \rightarrow S_3$ to $S_0 \rightarrow S_7$ (Table 3) are of CT nature and have weak absorption intensity. They are buried beneath the more intensive transitions of the absorption spectrum of **9PA** (Fig. 1).

3.3. Fluorescence

The excitation of the pyridinium cation at any wavelength within the absorption spectrum leads to a weak ($\Phi_f = 0.03$) fluorescence at 420 nm (Fig. 1, Table 4) possessing a relatively large Stokes shift with respect to the weak long wavelength absorption shoulder ($\Delta\nu_{a\text{-}f} = 5600\,cm^{-1}$) and a long fluorescence lifetime (average decay time 5.39 ns). The

Table 3
The characteristics of the main electronic transitions[a] of **9PA** calculated by CNDO/S [14–21]

Transition characteristic	$S_0 \rightarrow S_1$	$S_0 \rightarrow S_2$	$S_0 \rightarrow S_8$
Transition energy (eV)	3.98	4.13	5.72
Oscillator strength	0.0198	0.1096	0.3388
Transition dipole orientation[b]	*x* axes	*x* axes	*z* axes
Main contributions in configuration interaction (coefficient)[c]	54 → 55 (0.9671)	53 → 55 (0.5034) 52 → 55 (−0.8078) 51 → 56 (−0.2602)	–
Assignment	**CT**	**LE** (Acr)	**LE** (Acr)

[a] The data of the forbidden transitions (From $S_0 \rightarrow S_3$ till $S_0 \rightarrow S_7$) which have CT nature are not shown.
[b] The orientation of the axes is shown in Fig. 2.
[c] The orbitals are shown in Fig. 3.

Table 4
Fluorescence parameters of **9PA** (ethanol, 298 and 151 K)

T (K)	λ_f (nm)	$\Delta\nu_{a\text{-}f}$ (cm^{-1})	Φ_f	$\langle\tau_f\rangle$ (ns)	$\tau_r = \langle\tau_f\rangle / \Phi_f$ (ns)
298	420	5600	0.030	5.39[a]	179.1
151	420	5600	0.023	4.64	201.7

[a] At 303 K.

fluorescence excitation spectrum (Fig. 1) conforms well with the absorption spectrum. The position of the fluorescence band does not change with cooling of the solution from room temperature to 144 K. The variation of the fluorescence quantum yield with cooling is very small (Fig. 4).

The large value of the Stokes shift at 296 K cannot be caused by the orientation relaxation of the polar solvent molecules [28] because the position of the fluorescence and absorption bands for the different cations (in particular, the pyridinium cation) [27,29] depends weakly on the solvent polarity. Therefore, the large Stokes shift can be caused only by a large structural change from the equilibrium ground state geometry to the S_1 state equilibrium geometry. The most probable adiabatic geometry changes of **9PA** are phenyl rotation to a more planar geometry or bond length changes in the perpendicular geometry. An estimation of the radiative lifetime of the S_1 state ($\tau_r \approx 180$ ns, Table 4) from the fluorescence quantum yield and average lifetime shows that the emission as well as the long wavelength absorption band is connected with a forbidden transition, and therefore the emitting structure is also highly twisted (near orthogonal).

The influence of temperature on the photophysics is small. The absence of a fluorescence band shift by cooling of the solution suggests that the solvent environment has only a weak influence on the adiabatic geometry changes and, therefore, the emission occurs from near the twisted equilibrium structure at any temperature. In this case, the slight decrease of the fluorescence quantum yield with temperature (Fig. 4) could be caused by an increased radiative lifetime at lower temperature ($1/\Phi_f = 1 + \tau_r k_{nr}$). This proposal is supported by an estimation of the radiative lifetime at 151 K ($\tau_r = 204$ ns) (Table 4). A comparison of the results obtained for the radiative lifetime at various temperatures shows that the emitting structure at 151 K is characterized by a more forbidden transition than the emitting one at 298 K. Therefore, it can be supposed that a less perpendicular average fluorescent structure at 298 K (as compared to low temperature) is generated from the initial structure with near orthogonal fragments owing to larger librations of the 9-phenyl ring. The observation of an increase of the radiative rate constant with temperature is typical for charge transfer systems with near-perpendicular geometries and can be understood with a model of broadened rotational distribution functions around the perpendicular geometry [30].

3.4. Calculated excited state potential of **9PA**

For an estimation of possible relation processes in the singlet excited state of **9PA**, the vertical region of the potential of the S_1 state can be obtained by addition of the S_0-S_1 transition energy to the energy of the optimized S_0 state for different torsional angles between the cation fragments. The results show that the S_1 state possesses a considerably flatter potential for internal rotation than the S_0 state (Fig. 5). There is even some indication that the 90° minimum of the S_0 state shift to around 55° in S_1. This geometry with 55° is characterized by much more allowed transition (oscillator

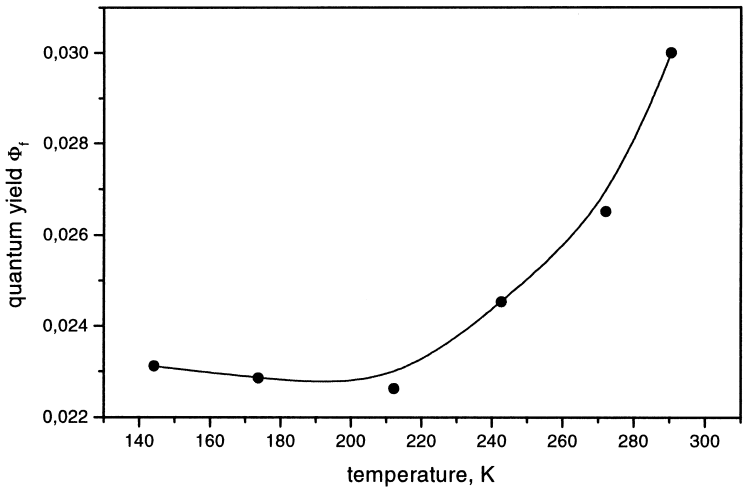

Fig. 4. Temperature dependence of the fluorescence quantum yield of **9PA** in ethanol.

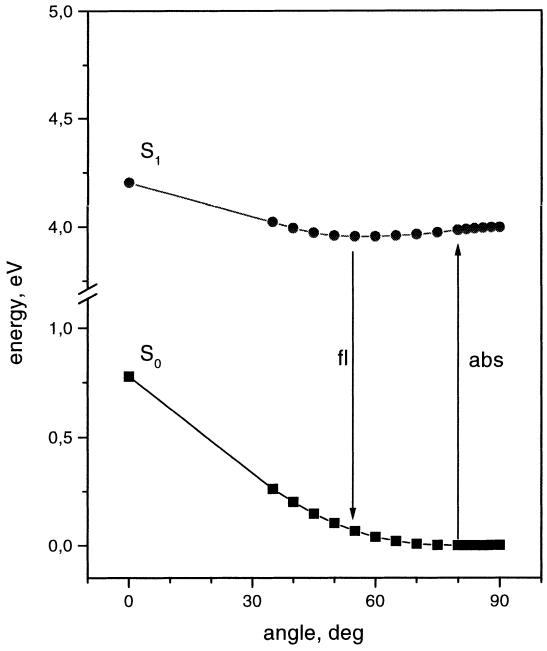

Fig. 5. Potential energy surfaces of internal rotation for **9PA** in the S_0- and S_1-state as calculated by AM1 and CNDO/S.

strength is 0.124) that is not correlated with the experimental observation of the forbidden character of the transition. Therefore, we propose that in fact the S_1 state equilibrium geometry is on average less twisted than the S_0 state equilibrium one but that the difference is weak and the torsional angle is around 75–80° corresponding to the observed forbidden transition. The data of the estimation for the excited state potential can be verified by an initial calculation of the S_1- and T_1-states for more simple model cations such as 4-phenyl-3,5-di-methyl-pyridinium.

4. Conclusions

The observation of a strongly forbidden absorption transition of CT-type from a sterically hindered 9-phenyl pyridinium cation in conjunction with forbidden emissive transition and with a relatively large Stokes shift indicates adiabatic geometry changes connected with the hindered rotation of the 9-phenyl ring. At the same the time marked contribution in the Stokes shift may be connected also with bond length changes or derivations from planarity of the rings brought about by the strong change of electronic distribution in the CT state.

Acknowledgements

The authors are grateful to the International Association for promotion of co-operation with scientists from the New Independent States of the former Soviet Union (INTAS grant N 96-1485) and to the Volkswagen Stifung for financial support.

References

[1] Y.R. Tymyansky, M.I. Knyazhansky, V.M. Feigelman, V.A. Kharlanov, Zh. Prikl. Spectr. (1985) 574.
[2] M.I. Knyazhansky, Y.R. Tymyansky, V.M. Feigelman, A.R. Katritzky, Heterocyles 26 (1987) 2963.
[3] M.I. Knyazhansky, V.A. Kharlanov, Y.R. Tymyansky, J. Photochem. Photobiol. A: Chem. 118 (1998) 151.
[4] V.A. Kharlanov, W. Rettig, M.I. Knyazhansky, N.I. Makarova, unpublished.
[5] G.N. Dorofeenko, Y.A. Zdanov, G.I. Shungijetu, S.W. Krivun, Tetrahedron 22 (1966) 1821.
[6] V.A. Kharlanov, W. Rettig, M.I. Knyazhansky, N.I. Makarova, J. Photochem. Photobiol. A: Chem. 103 (1997).
[7] I. Berlman, Handbook of Fluorescence Spectra of Aromatic Molecules, 2nd ed., Academic Press, New York, London, 1971.
[8] J.B. Birks, Photophysics of Aromatic Molecules, Wiley/Interscience, New York, 1970.
[9] J.A. Riddick, W.B. Bunger, Organic Solvents, Wiley/Interscience, New York, 1980.
[10] R. Passerini, J.G. Ross, J. Scient. Instr. 30 (1953) 274.
[11] M. Vogel, W. Rettig, Ber. Bunsenges, Phys. Chem. 91 (1987) 1241.
[12] M.J.S. Dewar, E.G. Zoebisch, E.F. Healy, J.J.P. Stewart, J. Am. Chem. Soc. 107 (1985) 3202.
[13] M.J.S. Dewar, J.J.P. Stewart, J.M. Ruiz, D. Liotard, E.F. Healy, R.D. Dennington II, AMPAC 5.0, Semichem, Shawnee, 1994.
[14] J. Del Bene, H.H. Jaffe, J. Phys. Chem. 48 (1968) 1807.
[15] J. Del Bene, H.H. Jaffe, J. Phys. Chem. 48 (1968) 4050.
[16] J. Del Bene, H.H. Jaffe, J. Phys. Chem. 49 (1968) 1221.
[17] J. Del Bene, H.H. Jaffe, J. Phys. Chem. 50 (1969) 1126.
[18] H.M. Chang, H.H. Jaffe, C.A. Masmanidis, J. Chem. Phys. 79 (1975) 1109,1118.
[19] J. Del Bene, J. Am. Chem. Soc. 95 (1973) 6517.
[20] J. Del Bene, J. Chem. Phys. 62 (1975) 666.
[21] J. Del Bene, J. Chem. Phys. 62 (1975) 1961.
[22] M.E. Kosower, P.E. Klinedinst, J. Am. Chem. Soc. 78 (1956) 3493.
[23] M.E. Kosower, S.W. Bauer, J. Am. Chem. Soc. 82 (1960) 2191.
[24] G.V. Tishenko, E.G. Protsenko, B.G. Distanov, Khim. Heter. Soed. (1973) 359 (Russian Chem. Heterocycl. Comp.).
[25] A. Katritzky, D. Lamba, R. Spagna, A. Vaciago, R. Prevo, J.H. Bieri, J.J. Stezowski, G. Musumarra, J. Chem. Soc. Perkin Trans. 2 (1987) 1391.
[26] S.M. Aldoshin, Y.R. Tymyansky, O.A. D'yachenko, L.O. Atovmyan, M.I. Knyazhansky, G.N. Dorofeenko, Izvet. AN SSSR, Ser. Khim. (1981) 2270.
[27] V.A. Kharlanov, M.I. Knyazhansky, W. Rettig, J. Mol. Struct. 380 (1996) 113.
[28] N.G. Bakhshiev, Spectroscopy of Intermolecular Interactions, Nauka, Moscow, 1972.
[29] V.A. Kharlanov, M.I. Knyazhansky, J. Photochem. Photobiol., A: Chem., in press.
[30] M. Van der Auweraer, Z.R. Grabowski, W. Rettig, J. Phys. Chem. 95 (1991) 2093.